



## LOW TEMPERATURE AND HIGHLY EFFICIENT OXIDATION OF SOOT BY O<sub>2</sub> OVER RU-BASED CATALYSTS IN FLUIDIZED BED REACTOR

Mingxin Guo, Lu Qiu\*

Feng Ouyang\*

**Abstract:** *The potentiality of Ru-based catalysts for soot oxidation by O<sub>2</sub> in fluidized bed reactor has been conducted with temperature programmed reaction (TPR) technique. Compared to Pt/SiO<sub>2</sub>, Ru/SiO<sub>2</sub> exhibited a higher activity in fixed bed reactor. The catalytic activity increased further after other metal oxides loading as second carrier. Among the Ru/MO<sub>x</sub>/SiO<sub>2</sub> (M=Al, Zr, Ti), Ru/TiO<sub>2</sub>/SiO<sub>2</sub> showed the highest activity and its T<sub>50</sub> decreased to 435 °C, which was 83 °C lower than Ru/SiO<sub>2</sub>. Two types of active sites, Ru<sub>x</sub>Ti<sub>(1-x)</sub>O<sub>2</sub> and RuO<sub>x</sub>, have been identified on the surface of Ru/TiO<sub>2</sub>/SiO<sub>2</sub>. Low temperature calcination for Ru/TiO<sub>2</sub>/SiO<sub>2</sub> produced the well-dispersed active sites and benefited the soot oxidation. Compared with fixed bed reactor, Ru-based catalysts are capable of lowering considerably soot combustion temperature in fluidized bed reactor. T<sub>50</sub> of the soot oxidation reaction over Ru/TiO<sub>2</sub>/SiO<sub>2</sub> decreased to 389 °C. The increase in soot oxidation efficiency at low temperature active sites in the fluidized bed reactor is attributed to the easier migration of activated oxygen species between gas and solid since fluidization improved mass transfer.*

**Keywords:** *Soot oxidation; Fluidized bed reactor; Ruthenium; Metal oxides; Oxygen*

\*Environmental Science and Engineering Research Center, Harbin Institute of Technology  
Shenzhen Graduate School, Shenzhen, P.R.China



## 1. INTRODUCTION

Soot emitted from the diesel engines as an unwelcome byproduct can cause serious environmental problems and it presents a respiratory hazard as it often contains adsorbed PAH. In addition, unburned hydrocarbon molecules, several of which show mutagenic or carcinogenic characteristics, condense on the surface of the soot. Because of these diverse implications, research on the removal of soot from diesel exhaust gas has scattered. Among various technical approaches for the control of soot emission, the direct and much valid way is to place a diesel particulate filter (DPF) in the exhaust stream, which needs to clean the accumulation periodically by combustion or oxidation in order to prevent pressure increase. Under normal exhaust gas conditions, the oxidation or combustion reactivity of soot is low. Therefore, the use of a catalyst that will ensure acceptable oxidation rates at low temperature is preferred. In recent years, many catalysts for soot oxidation have been reported, such as metal oxides [1-10], precious metals [11-17] and the combined systems [18-20]. Among them, precious metals catalysts exhibit high activity, and some researches on the soot oxidation over platinum have been reported. Aouad *et al.* [21-23] have reported that Ru/CeO<sub>2</sub> shows high activity in the oxidations of soot and volatile organic compounds. They found that ruthenium was present in RuO<sub>2</sub> state and took an important role in the oxidation of soot. RuO<sub>4</sub> that is highly volatile only may be formed above 730°C. Aouad *et al.* [22] also examined the reactivity of soot over Ru/CeO<sub>2</sub> by repeated experiments and regarded as no ruthenium loss because the activity of the catalyst did not decrease even after 10 cycles of carbon particles oxidation. Hence, it is possible and important for Ru-based catalysts used for the soot oxidation. However, little work has been done systematically about the Ru-based catalysts.

It is verified in earlier work [2] that the contact between catalyst and soot is an important factor for the soot oxidation. When this contact is poor ('loose contact'), the activity of catalyst is much lower than when the contact is 'tight contact'. Unfortunately, the contact between catalyst and carbon particles is poor and comparable with loose contact under practical conditions in a classical filter. Thus, improvement of contact between soot and catalyst under practical operations is of great importance. However, most of experiments



about simulated soot oxidation were conducted in fixed bed reactor. The oxidation of soot in fluidized bed reactor which has excellent heat and mass transfer characteristics has almost not been reported [24]. It must be noted that the use of fluidized bed may avoid pore blocking on honeycomb catalyst which is used generally as support because of un-burning soot accumulation in fixed bed.

In this work, we investigate the soot oxidation over Ru-based catalysts in fluidized bed reactor, and carry out an exploratory research about the activities of a series of Ru-based catalysts and the effect of supports.

## 2. EXPERIMENTAL

### 2.1. Catalyst Preparation

Ru/SiO<sub>2</sub> catalyst was prepared by iso-volumetric impregnation of SiO<sub>2</sub> (Qingdao Haiyang Chemical Co., Ltd, 354 m<sup>2</sup>/g) with an aqueous solution of RuCl<sub>3</sub>·nH<sub>2</sub>O (Platinum Group Metals China), and left for one day at room temperature. The impregnated catalyst precursor was then dried in air at 110°C for 12 h, followed by calcination in air at 500°C for 3h. For comparison, Pt/SiO<sub>2</sub> catalyst was also prepared with an aqueous solution of H<sub>2</sub>PtCl<sub>6</sub>·nH<sub>2</sub>O. Metal oxides (M=Al, Zr, Ti) were loaded onto SiO<sub>2</sub> to prepare MO<sub>x</sub>/SiO<sub>2</sub> (M=Al, Zr, Ti) by the iso-volume impregnation using metal salts (Al(NO<sub>3</sub>)<sub>3</sub>·9H<sub>2</sub>O, Zr(NO<sub>3</sub>)<sub>4</sub>·5H<sub>2</sub>O and Ti(SO<sub>4</sub>)<sub>2</sub>) as precursors, left for one day at room temperature, followed by dried in air at 110°C for 12 h and calcination at 500°C in air for 3 h. Ruthenium was supported on these oxides, which were preloaded onto SiO<sub>2</sub>, same as the preparation of Ru/SiO<sub>2</sub> mentioned above. Therefore, Ru/MO<sub>x</sub>/SiO<sub>2</sub> (M=Al, Zr, Ti) samples were prepared. In the experiment about the crystallinity and catalytic activities of TiO<sub>2</sub>/SiO<sub>2</sub> and Ru/TiO<sub>2</sub>/SiO<sub>2</sub>, catalysts were calcined at 550-700°C for 3 h. For all the catalysts, the noble metal loading was 1wt. % and the metal oxides were 10 wt. %.

### 2.2. Catalyst Activity Measurement

Catalytic activity was measured with temperature programmed reaction (TPR) technique. The experiments were carried out in a quartz microreactor (9mm of i.d.) that can be operated in either fluidized bed or fixed bed mode. The perforated plate and filter were added in the middle region of the microreactor. The height of fluidized bed is 20 mm. The



reactor temperature was monitored with a thermocouple and controlled by PID-regulation system (Bachy, CKW-2200). The temperature was raised at a rate of  $1^{\circ}\text{C}/\text{min}$  from  $150^{\circ}\text{C}$  to  $600^{\circ}\text{C}$ . After separating through a Porapak Q column and converting to methane over a Ni catalyst at  $360^{\circ}\text{C}$ , the concentrations of CO and  $\text{CO}_2$  were measured with an on-line gas chromatograph (Shimadzu, Japan, GC-2014C), equipped with a flame ionization detector (FID).

Printex-U (Degussa AG;  $100\text{ m}^2/\text{g}$ ) was used as model soot for the activity measurement which is similar to literature [1]. The carbon particles were sieved with screen of 40 and 60 mesh/inch<sup>2</sup>. Catalysts particles were sieved with 60 and 100 mesh/inch<sup>2</sup> and medium size particles were used for the activity measurement in fixed and fluidized bed reactors. The catalyst granules (0.2 g) and model soot (0.02 g) were carefully mixed with spatula and held on the perforated plate in the microreactor. Mixing in this way resulted in a “loose” contact between the catalyst and soot, which was assumed to be similar with that found in practice cases [2]. The height of catalyst and carbon particle mixture in fixed bed reactor was about 12mm. The reaction gas which contained  $\text{O}_2$  (4.4 vol%) with Ar as the balance gas, was fed through the catalyst bed at a rate of 150 ml/min.

For the deactivation experiment of catalysts, similar to the description above, the only difference was that soot was added into the catalyst used last time and mixed, then held on the perforated plate in the microreactor.

The catalytic activity was evaluated by temperature of soot oxidation and selectivity to CO throughout a TPR run. The values of  $T_{10}$ ,  $T_{50}$ , and  $T_{90}$  were defined as the temperatures, at which 10%, 50% and 90% carbon particles were oxidized during the TPR run. The selectivity of carbon monoxide ( $S_{\text{CO}}$ , %) was calculated by the ratio of CO to the sum of CO and  $\text{CO}_2$  in a TPR run. The removal rate of soot (%) was calculated by the ratio of  $\text{CO}_x$  ( $=\text{CO}+\text{CO}_2$ ) to the  $\text{CO}_x$  that soot was oxidized completely.

### 2.3 Characterization of the Catalyst

$\text{N}_2$  adsorption-desorption isotherms (at  $-196^{\circ}\text{C}$ ) were used for the determination of surface area (BET method), pore volume and average pore diameter of the samples (Table 1). Each catalyst was introduced in a quartz cell, followed by degassing at  $300^{\circ}\text{C}$  in vacuum for 3h,



finally measured for the desired adsorption parameters using the Belsorp II apparatus.

Hydrogen temperature programmed reduction experiments (H<sub>2</sub>-TPR) were performed in a flow type reactor. Hydrogen (5 vol.% in N<sub>2</sub>) was passed through a reaction tube containing samples at 30 ml/min. The tube was heated with an electric furnace at a rate of 5°C/min from room temperature to 600°C, and the amount of hydrogen consumed was monitored with a TCD detector. The H<sub>2</sub>O produced by the reduction process was trapped before the TCD.

The morphologies of the catalysts were observed by transmission electron microscopy (TEM, JEOL, JEM-2010) at an acceleration voltage of 200 kV. The samples were dispersed ultrasonically in ethanol and deposited on a holey carbon copper grid before measurement.

The crystalline structures of the fresh catalysts were determined by X-ray diffractometer (Rigaku D/max 2500PC), using Cu K $\alpha$ 1 radiation combined with Nickel filter operating at 40kV and 200mA. The diffraction data were recorded for 2 $\theta$  values between 20° and 80° with a scanning rate of 6°/min.

### 3. RESULTS AND DISCUSSION

#### 3.1. Effect of Ruthenium

In Fig.1, the catalytic performance of SiO<sub>2</sub> is compared with that of Ru/SiO<sub>2</sub>. The SiO<sub>2</sub> did not show any oxidation activity until 480°C. Above 480°C, soot was oxidized moderately. Broad change of the profile with the increased temperature indicated that the reaction or active sites on the SiO<sub>2</sub> were not homogeneous even under fluidized bed condition. The reaction was finished at 580°C and CO selectivity was about 20% during the TPR reaction. On the other hand, the oxidation over Ru/SiO<sub>2</sub> was initiated at 430°C and finished at 490°C. These temperatures are 50°C lower than those of SiO<sub>2</sub>. The sharp peak in TPR profile of Ru/SiO<sub>2</sub> shows the rapid reaction once the reaction started. The strong oxidation property of Ru/SiO<sub>2</sub> led to lower CO selectivity of 7%.

T<sub>90</sub> of soot oxidation over Ru/SiO<sub>2</sub> in fluidized bed reactor is 488°C far lower than 730°C only above which RuO<sub>4</sub> may be formed. Therefore, the hazard from the volatility of ruthenium oxides may be ignored in our experiment.



### 3.2. Effect of Support Oxide

The catalytic activities of a series of Ru-based catalysts and corresponding support oxides for soot oxidation in fluidized bed reactor are tabulated in Table 2.  $T_{10}$ ,  $T_{50}$ ,  $T_{90}$  of  $\text{MO}_x/\text{SiO}_2$  (M=Al, Zr and Ti) samples are slightly higher or close to those of  $\text{SiO}_2$  in fluidized bed reactor, which demonstrates that  $\text{MO}_x$  (M=Al, Zr and Ti) supported on  $\text{SiO}_2$  without noble metals have little promoted effect on the activity of soot oxidation. Compared to  $\text{SiO}_2$ , the CO selectivity of  $\text{MO}_x/\text{SiO}_2$  increased evidently. This suggests that  $\text{MO}_x$  supported on  $\text{SiO}_2$  without noble metals hindered the complete oxidation of soot but benefited the partial oxidation of soot to CO.

After loading ruthenium, the activity of  $\text{Ru}/\text{TiO}_2/\text{SiO}_2$  is the highest and the  $T_{10}$ ,  $T_{50}$ ,  $T_{90}$  of soot oxidation is  $360^\circ\text{C}$ ,  $389^\circ\text{C}$  and  $414^\circ\text{C}$  in sequence. These temperatures are  $70\text{-}90^\circ\text{C}$ ,  $110\text{-}170^\circ\text{C}$  and  $130\text{-}200^\circ\text{C}$  lower than those of  $\text{Ru}/\text{SiO}_2$ ,  $\text{SiO}_2$  and  $\text{TiO}_2/\text{SiO}_2$ , respectively. Moreover, the activity of  $\text{Ru}/\text{MO}_x/\text{SiO}_2$  is in order:  $\text{Ru}/\text{TiO}_2/\text{SiO}_2 > \text{Ru}/\text{Al}_2\text{O}_3/\text{SiO}_2 > \text{Ru}/\text{SiO}_2 > \text{Ru}/\text{ZrO}_2/\text{SiO}_2$ . Since  $\text{MO}_x/\text{SiO}_2$  samples do not enhance the activity of soot oxidation, we suggest that ruthenium is regarded as an active component and responsible for the formation of active oxygen species, whereas metal oxides  $\text{MO}_x$  act as the oxygen species or CO acceptor to benefit soot oxidation.

The removal activity of soot over  $\text{Ru}/\text{TiO}_2/\text{SiO}_2$  calcined at different temperatures in fluidized bed reactor is plotted in Fig.2. It should be noted that the combustion temperature of soot over  $\text{Ru}/\text{TiO}_2/\text{SiO}_2$  calcined at  $500^\circ\text{C}$  in fluidized bed reactor is about  $100^\circ\text{C}$  lower than other samples.  $\text{Ru}/\text{TiO}_2/\text{SiO}_2$  samples calcined at  $550^\circ\text{C}$ ,  $600^\circ\text{C}$ ,  $650^\circ\text{C}$  and  $700^\circ\text{C}$  have close  $T_{50}$  values around  $490^\circ\text{C}$ . The  $\text{Ru}/\text{TiO}_2/\text{SiO}_2$  samples (except for  $500^\circ\text{C}$ ) lost their high activity may be related to the changes of active components, such as  $\text{Ru}_x\text{Ti}_{(1-x)}\text{O}_2$  [25],  $\text{RuO}_2$  and  $\text{RuO}_{2-x}$  [26-28], in crystal structures, dispersed properties and oxidation-reduction nature.

Taking in consideration for the application and volatility of ruthenium supported on  $\text{TiO}_2/\text{SiO}_2$ , the catalyst life has been tested and reaction experiments were repeated with the same catalyst for 4 TPR circle runs. The percentage of soot removal as a function of temperature is plotted in Fig.3. From Fig.3, the removal curves of soot over  $\text{Ru}/\text{TiO}_2/\text{SiO}_2$  in



fluidized bed reactor are similar.  $T_{10}$ ,  $T_{50}$  and  $T_{90}$  for the 1st TPR, 2nd TPR and 4th TPR runs are about  $360^{\circ}\text{C}$ ,  $390\text{-}400^{\circ}\text{C}$  and  $410\text{-}420^{\circ}\text{C}$ , respectively. This gives an important implication for the application of Ru/TiO<sub>2</sub>/SiO<sub>2</sub> because it is still active during the fourth TPR run as the fresh catalyst in the first TPR run. This repeated experiment also indicated that ruthenium oxides formed on Ru/TiO<sub>2</sub>/SiO<sub>2</sub> were not volatile under our experimental condition because there was no deactivation after several TPRs.

### 3.3 Comparison between Ruthenium and Platinum

Fig.4 shows the TPR profiles of Ru/SiO<sub>2</sub> and that of Pt/SiO<sub>2</sub> in fluidized bed reactor.  $T_{10}$ ,  $T_{50}$  and  $T_{90}$  of soot oxidation over Pt/SiO<sub>2</sub> are  $466^{\circ}\text{C}$ ,  $549^{\circ}\text{C}$  and  $580^{\circ}\text{C}$ , respectively. These temperatures are  $33^{\circ}\text{C}$ ,  $74^{\circ}\text{C}$  and  $92^{\circ}\text{C}$  higher than those of Ru/SiO<sub>2</sub>. The TPR profile of Pt/SiO<sub>2</sub> is broad and the CO selectivity is about 7%.

It has been verified that the presence of NO + O<sub>2</sub> in the feed gas promoted more efficiently the oxidation of soot than only O<sub>2</sub> in the feed gas [29, 30], because NO<sub>2</sub> produced by oxidization of NO over catalyst was a stronger oxidizer than O<sub>2</sub>. Oi-Uchisawa *et al.* [31] investigated the oxidation of soot over various Pt/MO<sub>x</sub>/SiC catalysts in fixed bed reactor and the feed gas contained 1000 ppm NO, 100 ppm SO<sub>2</sub>, 7% H<sub>2</sub>O and 10% O<sub>2</sub> balanced with N<sub>2</sub> at a flow rate of 500ml/min. They [11] also explained the mechanism of soot oxidation in the presence of O<sub>2</sub>, NO, SO<sub>2</sub> and H<sub>2</sub>O over Pt catalysts. They found that SO<sub>3</sub> (or H<sub>2</sub>SO<sub>4</sub>) produced from SO<sub>2</sub> acted as a catalyst to accelerate soot oxidation by NO<sub>2</sub> in the presence of H<sub>2</sub>O.  $T_{50}$  and  $T_{90}$  obtained are  $427^{\circ}\text{C}$  and  $521^{\circ}\text{C}$  for the soot oxidation over the catalyst [31], which is under more beneficial conditions than our experiment.  $T_{50}$  and  $T_{90}$  are  $398^{\circ}\text{C}$  and  $421^{\circ}\text{C}$  in our experiment. These are  $30^{\circ}\text{C}$  and  $100^{\circ}\text{C}$  lower than those reported by Oi-Uchisawa *et al.*, respectively [31]. Hence, Ru-based catalyst is more suitable for soot oxidation than the Pt loading catalyst.

### 3.4 Characteristics of Ru/TiO<sub>2</sub>/SiO<sub>2</sub>

TiO<sub>2</sub>/SiO<sub>2</sub> and Ru/TiO<sub>2</sub>/SiO<sub>2</sub> calcined at different temperatures were prepared to study crystal structures of the catalysts. X-ray diffraction patterns of TiO<sub>2</sub>/SiO<sub>2</sub> calcined at  $500^{\circ}\text{C}$ ,  $600^{\circ}\text{C}$  and  $700^{\circ}\text{C}$  or Ru/TiO<sub>2</sub>/SiO<sub>2</sub> calcined at  $500^{\circ}\text{C}$ ,  $550^{\circ}\text{C}$ ,  $600^{\circ}\text{C}$ ,  $650^{\circ}\text{C}$  and  $700^{\circ}\text{C}$  are exhibited in Fig.5, respectively. For the TiO<sub>2</sub>/SiO<sub>2</sub> calcined at  $500^{\circ}\text{C}$  a broad peak at around





22° exhibits that amorphous SiO<sub>2</sub> is present, but crystalline TiO<sub>2</sub> is not observed. After thermal treatment at 600°C and 700°C, a strong characteristic diffraction peak exists at 25°. The peak reveals the formation of anatase as a main crystalline phase in TiO<sub>2</sub>/SiO<sub>2</sub> [32, 33], while rutile was formed hardly even at high temperature of 700°C. For Ru/TiO<sub>2</sub>/SiO<sub>2</sub> calcined at 500°C, two very weak peaks, one belonging to anatase at 25° and the other being similar to RuO<sub>2</sub> structure at 28°, appeared. This indicated that the catalyst calcined at 500°C was well dispersed. When the pretreatment temperature increased from 550°C to 700°C, the peaks at 28° and 35° became apparent, which has been assigned to RuO<sub>2</sub> [26]. Meanwhile, rutile-type Ti oxide was confirmed to be formed by small peaks at 27° and 36° [33-36]. The XRD diffraction peaks of anatase, rutile-type Ti as well as Ru oxides decreased suddenly in intensity when the calcination temperature rose from 500°C to 550°C, while catalyst samples calcination at 550°C, 600°C and 650°C almost did not cause any change in intensity besides a little widening of 36° peaks for the catalyst calcined at 550°C. Compared with Ru/TiO<sub>2</sub>/SiO<sub>2</sub> calcined above 550°C, we suggest that Ru and Ti oxides in the catalyst calcined at 500°C are in well-dispersed state. On the other hand, after calcination above 550°C, various components were separated out to form crystalline anatase, rutile-type Ti and Ru oxides.

H<sub>2</sub>-TPR profiles of SiO<sub>2</sub>, TiO<sub>2</sub>/SiO<sub>2</sub>, Ru/SiO<sub>2</sub> and Ru/TiO<sub>2</sub>/SiO<sub>2</sub> samples are shown in Fig.6. There is no hydrogen consumption peak in SiO<sub>2</sub>. However, two hydrogen consumption peaks at around 510°C and 620°C for TiO<sub>2</sub>/SiO<sub>2</sub> are observed, respectively. The high-temperature peaks present in the H<sub>2</sub>-TPR measurement of TiO<sub>2</sub>/SiO<sub>2</sub> could be eventually assigned to the reduction of the support (Ti<sup>4+</sup>→Ti<sup>3+</sup>) [37]. It is well-known that TiO<sub>2</sub> is partially reduced to TiO<sub>2-x</sub> by hydrogen at high temperatures (above 500°C) and this process is promoted by the presence of dispersed metal crystallites [38, 39]. Rodríguez-González *et al.* [40] reported a H<sub>2</sub>-TPR result from Au/TiO<sub>2</sub> and a small hydrogen consumption peak at around 480°C was associated with the reduction of superficial Ti<sup>4+</sup> to Ti<sup>3+</sup>. In our ruthenium-containing catalysts, hydrogen consumption peaks appeared at around 180°C and 205°C. The former are attributed to the partial reduction of Ru species from RuO<sub>2</sub> to Ru<sup>0</sup>, referred as RuO<sub>x</sub> [26-28]. On Ru/SiO<sub>2</sub>, the latter is also observed, indicating the formation of RuO<sub>2</sub> on SiO<sub>2</sub>.





Nevertheless, the amounts of formed  $\text{RuO}_2$  are different between  $\text{Ru/SiO}_2$  and  $\text{Ru/TiO}_2/\text{SiO}_2$ . On the  $\text{Ru/SiO}_2$ ,  $\text{RuO}_2$  was dominant species, while  $\text{RuO}_x$  was main species on  $\text{Ru/TiO}_2/\text{SiO}_2$  calcined at  $500^\circ\text{C}$ . Thus, we suggest that the interaction of Ru with Ti species benefited the formation of  $\text{RuO}_x$ . Another strong and broad peak at around  $315^\circ\text{C}$  is observed on  $\text{Ru/TiO}_2/\text{SiO}_2$  catalyst, whereas this peak is not present on  $\text{Ru/SiO}_2$ . Moreover, compared to  $\text{Ru/SiO}_2$ , Ru was decreased largely on  $\text{Ru/TiO}_2/\text{SiO}_2$ . The lost Ru must be well dispersed to the surface or body phase of  $\text{TiO}_2$  particle. Rizzi *et al.* [25] have suggested that partial Ru may dope into  $\text{TiO}_2$  to form  $\text{Ru}_x\text{Ti}_{(1-x)}\text{O}_2$  surface solid solution, which is one of well-dispersed forms to contribute the peak area at  $315^\circ\text{C}$  in  $\text{Ru/TiO}_2/\text{SiO}_2$ . Compared with  $\text{TiO}_2/\text{SiO}_2$ , a large increase in the alone peak area suggests the formation of  $\text{Ru}_x\text{Ti}_{(1-x)}\text{O}_2$  surface solid solution that enhances hydrogen reduction.

TEM observation was also performed in Ru-based catalysts to examine the dispersion and morphologies of supported Ru particles (Fig. 7). We observe that Ru-based catalysts particle size is very small, close to about 5nm. Although ruthenium could be not identified with TEM, the observation for about 5nm of particles demonstrates that Ru and Ti oxides on  $\text{SiO}_2$  were well dispersed, as shown in Fig.5. The observation is consistent with  $\text{H}_2$ -TPR results, in which there are only two types of well-dispersed active components on  $\text{Ru/TiO}_2/\text{SiO}_2$ .

TPR profiles of the soot oxidation over  $\text{Ru/TiO}_2/\text{SiO}_2$  samples calcined from  $500^\circ\text{C}$  to  $700^\circ\text{C}$ , as shown in Fig. 2, are corresponding to X-ray diffraction patterns of  $\text{Ru/TiO}_2/\text{SiO}_2$  calcined at different temperatures exhibited in Fig.5. The oxidation activity of the  $\text{Ru/TiO}_2/\text{SiO}_2$  calcined at  $500^\circ\text{C}$  is different from these calcined at the other temperatures.  $T_{50}$  of  $\text{Ru/TiO}_2/\text{SiO}_2$  calcined at  $500^\circ\text{C}$  is  $390^\circ\text{C}$ , while  $T_{50}$ s of the other samples are near  $490^\circ\text{C}$ . This is corresponding to the change of Ru oxide forms. In  $\text{Ru/TiO}_2/\text{SiO}_2$  calcined at  $500^\circ\text{C}$ , the Ru oxides were well dispersed and benefited the soot oxidation in fluidized bed reaction. However, when the catalyst was calcined at  $550^\circ\text{C}$ ,  $600^\circ\text{C}$ ,  $650^\circ\text{C}$  and  $700^\circ\text{C}$ , the precipitation amounts of crystalline  $\text{RuO}_2$  are almost close to each other for samples calcined above  $550^\circ\text{C}$ , the decreased amounts in activity are also similar. Thus, we believe that crystalline  $\text{RuO}_2$  for soot oxidation is a low active component. This is in good agreement with the results shown in Fig.6 and Fig.7. Based on observation with TEM, well-dispersed particles



are nano size order. Apparently, the well-dispersed nano particles have higher reactivity in the present reaction than perfected crystal particles by heating treatment above 550°C. Because oxygen defects are generated easily on nanoparticles surface where active oxygen can be formed by adsorption, the catalysts in well-dispersed state benefit the oxygen provision which is one of important activity-control factors for soot catalytic oxidation reaction.

### 3.5 Comparison of Soot Oxidation between Fluidized and Fixed Bed Reactors

Fig.8 displays TPR profiles of soot oxidation over Ru/SiO<sub>2</sub> and Ru/TiO<sub>2</sub>/SiO<sub>2</sub> calcined at 500°C in fluidized and fixed bed reactors. From this figure and table 2 which also contains catalytic activity data from fluidized bed reaction as well as fixed bed reaction, a number of results should be noted. Firstly, Ru/TiO<sub>2</sub>/SiO<sub>2</sub> in the fluidized bed reactor is capable of lowering considerably the soot combustion temperature ( $T_{50}$ ) to 389°C. Secondly, the catalytic activity in the fixed bed reactor is always lower (resulting in higher combustion temperatures) than the activity in the fluidized bed reactor. The reduced temperature values are related to second support types. The higher the activity of catalyst, the larger the lowered temperature values are. For the same catalyst with the same amount, the difference in oxidation activities between fixed and fluidized should be attributed to mass transfer effect in the two reaction systems. Lastly, two peaks at 430°C and 445°C in profile for the fixed bed reaction are observed in figure 8, respectively, which means that two types of active sites were present on the catalyst. Nevertheless, a very interesting observation is that low temperature peak was most strong and shifted to 389°C during soot oxidation over Ru/TiO<sub>2</sub>/SiO<sub>2</sub> in fluidized bed. This demonstrates that soot oxidation occurred rapidly on low temperature active sites, and almost finished when the temperature was raised to 400°C. This shows that mass transfer is an important control step in the solid-solid reaction.

Oxygen is only possible activated gaseous species, moreover the presence of catalyst resulted in an increase in the reaction activity (Table 2). Hence, soot oxidation must involve in oxygen activation by the catalysts. The activated oxygen species are regarded as being capable of migration from catalyst to carbon particle, finally, reacting with it. From Table 2 we find that reaction temperatures related to Ru-based catalysts are lower in fluidized bed



reactor than in fixed bed reactor. Since the difference in both reactions is only in mass transfer, we suggest that the improvement of the mass transfer lead to an increase in the reaction activity.

On the other hand, broad characteristics in the profile of soot conversion above 450°C over SiO<sub>2</sub> and Pt/SiO<sub>2</sub> are observed in fluidized bed reactor, indicating heterogeneity of the reactions or low activities of the catalysts (Figs 1 and 4). In addition, broad characteristic in the profile of the carbon conversion over Ru/SiO<sub>2</sub> in fixed bed reactor was also present in high temperature. Nevertheless, the broad characteristic disappeared, and a sharp peak at around 480°C appeared over the same Ru/SiO<sub>2</sub> samples in fluidized bed reactor. The sharp peak means that the reaction is uniform over the Ru/SiO<sub>2</sub>. Thus, the broad characteristic in reaction activity may be explained as heterogeneity of the reactions, which originates from heterogeneity of catalyst physical distribution. The latter means that contact form and distance between catalyst and soot are different in fixed bed reactor. For Ru/SiO<sub>2</sub>, it belongs to heterogeneity of the catalyst physical distribution. Thus migration is required for collision and reaction of these separated species. Because of heat uniform and better mass transfer under the condition of fluidization, probability of the reaction is much larger than that in the fixed bed reactor. After adding second carrier TiO<sub>2</sub>, performance of the catalyst was improved, and combustion temperature ( $T_{50}$ ) dropped down to 389°C over Ru/TiO<sub>2</sub>/SiO<sub>2</sub>. Additionally, two reaction peaks on Ru/TiO<sub>2</sub>/SiO<sub>2</sub>, corresponding to two types of active sites, appeared in fixed bed reactor. Nevertheless, the latter active site did not play an important role in fluidized bed reactor since the reaction has been completed efficiently on the first active site. A similar high efficiency was also observed on Ru/SiO<sub>2</sub>. Based on H<sub>2</sub>-TPR results, we have identified the two types of active components, RuO<sub>x</sub> and Ru<sub>x</sub>Ti<sub>(1-x)</sub>O<sub>2</sub> surface solid solution on Ru/TiO<sub>2</sub>/SiO<sub>2</sub>. However, it is not most clear for oxygen activation and transfer ways on RuO<sub>x</sub>, and Ru<sub>x</sub>Ti<sub>(1-x)</sub>O<sub>2</sub> because of complexity of solid-solid and gas-solid reactions in fluidized bed system. The related mechanisms are in study.

#### 4. CONCLUSION

The oxidation of carbon particles over Ru-based catalysts supported on SiO<sub>2</sub> was conducted in fluidized bed reactor, and Ru/SiO<sub>2</sub> showed higher activity for soot oxidation than Pt/SiO<sub>2</sub>.



The effect of second carriers on catalytic activity was examined.  $\text{MO}_x$  ( $M=\text{Al}, \text{Zr}, \text{Ti}$ ) supported by  $\text{SiO}_2$  showed low oxidation activity for carbon particle and benefited partial oxidation of soot to CO. After loaded ruthenium,  $\text{Ru}/\text{TiO}_2/\text{SiO}_2$  exhibits a big advantage among  $\text{Ru}/\text{MO}_x/\text{SiO}_2$  ( $M= \text{Al}, \text{Zr}$  and  $\text{Ti}$ ) for the oxidation of soot and the  $T_{10}$ ,  $T_{50}$ ,  $T_{90}$  of soot oxidation is  $360^\circ\text{C}$ ,  $389^\circ\text{C}$  and  $414^\circ\text{C}$ . Two types of ruthenium species are regarded as active components and responsible for formation of active oxygen species. Well dispersion of  $\text{RuO}_x$ , and  $\text{Ru}_x\text{Ti}_{(1-x)}\text{O}_2$  surface solid solution on  $\text{Ru}/\text{TiO}_2/\text{SiO}_2$  calcined at  $500^\circ\text{C}$  benefited the soot oxidation. However, crystalline Ru and Ti oxides formed on  $\text{Ru}/\text{TiO}_2/\text{SiO}_2$  calcined at higher temperature and lost the activity in soot oxidation. Because activated oxygen species are difficult to migrate in fixed bed reactor, the oxidation of carbon particles in different forms contact with catalyst particles requires higher reaction temperature than fluidized bed reactor. The reaction of soot occurred in lower temperature in fluidized bed reactor due to heat uniform and better mass transfer under fluidization condition.

## ACKNOWLEDGEMENT

This project is financially supported by Shenzhen commission of science and technology innovation (No. JCYJ20120613154128107), (No. JCYJ20140417172417138), and by The ministry of construction (No. 2008-k4-5).

## REFERENCES

- [1] Neeft J.P.A., Makkee M., Moulijn J.A. (1996). Catalysts for the Oxidation of Soot from Diesel Exhaust Gases. I. An Exploratory Study. *Applied Catalysis B: Environmental*, 8, 57-78.
- [2] Neeft J.P.A., van Pruissen O.P., Makkee M., Moulijn J.A. (1997). Catalysts for the Oxidation of Soot from Diesel Exhaust Gases. II. Contact between Soot and Catalyst under Practical Conditions. *Applied Catalysis B: Environmental*, 12, 21-31.
- [3] Neri G., Bonaccorsi L., Donato A., Milone C., Musolino M.G., Visco A.M. (1997). Catalytic Combustion of Diesel Soot over Metal Oxide Catalysts. *Applied Catalysis B: Environmental*, 11, 217-231.
- [4] Liu S., Obuchi A., Uchisawa J., Nanba T., Kushiyama S. (2002). An Exploratory Study of



- Diesel Soot Oxidation with  $\text{NO}_2$  and  $\text{O}_2$  on Supported Metal Oxide Catalysts. *Applied Catalysis B: Environmental*, 37, 309-319.
- [5] Leocadio I.C.L., Minana C.V., Braun S., Schmal M. (2008). Effect of experimental conditions on the parameters used for evaluating the performance of the catalyst  $\text{Mo}/\text{Al}_2\text{O}_3$  in diesel soot combustion. *Applied Catalysis B: Environmental*, 84, 843-849.
- [6] Aneggi E., de Leitenburg C., Dolcetti G., Trovarelli A. (2008). Diesel soot combustion activity of ceria promoted with alkali metals. *Catalysis Today*, 136, 3-10.
- [7] Reddy B.M., Rao K.N. (2009). Copper Promoted Ceria-zirconia Based Bimetallic Catalysts for Low Temperature Soot Oxidation. *Catalysis Communications*, 10, 1350-1353.
- [8] Liu J., Zhao Z., Lan J., Xu C., Duan A., Jiang G., Wang X. and He H. (2009). Catalytic Combustion of Soot over the Highly Active  $(\text{La}_{0.9}\text{K}_{0.1}\text{CoO}_3)_x/\text{nmCeO}_2$  Catalysts. *The Journal of Physical Chemistry C*, 113, 17114-17123.
- [9] Teraoka Y., Nakano K., Kagawa S., Shangguan W.F. (1995). Simultaneous Removal of Nitrogen Oxides and Diesel Soot Particulates Catalyzed by Perovskite-type Oxides. *Applied Catalysis B: Environmental*, 5, L181-L185.
- [10] Shangguan W.F., Teraoka Y., Kagawa S. (1998). Promotion Effect of Potassium on the Catalytic Property of  $\text{CuFe}_2\text{O}_4$  for the Simultaneous Removal of  $\text{NO}_x$  and Diesel Soot Particulate. *Applied Catalysis B: Environmental*, 16, 149-154.
- [11] Oi-Uchisawa J., Obuchi A., Zhao Z., Kushiyama S. (1998). Carbon Oxidation with Platinum Supported Catalysts. *Applied Catalysis B: Environmental*, 18, L183-L187.
- [12] Oi-Uchisawa J., Obuchi A., Ogata A., Enomoto R., Kushiyama S. (1999). Effect of Feed Gas Composition on the Rate of Carbon Oxidation with  $\text{Pt}/\text{SiO}_2$  and the Oxidation Mechanism. *Applied Catalysis B: Environmental*, 21, 9-17.
- [13] Oi-Uchisawa J., Obuchi A., Wang S., Nanba T., Ohi A. (2003). Catalytic Performance of  $\text{Pt}/\text{MO}_x$  Loaded over SiC-DPF for Soot Oxidation. *Applied Catalysis B: Environmental*, 43, 117-129.
- [14] Oi-Uchisawa J., Wang S., Nanba T., Ohi A., Obuchi A. (2003). Improvement of Pt Catalysts for Soot Oxidation Using Mixed Oxide as a Support. *Applied Catalysis B: Environmental*, 44, 207-215.



- [15] Hosoya M., Shimoda M. (1996), The Application of Diesel Oxidation Catalysts to Heavy Duty Diesel Engines in Japan. *Applied Catalysis B: Environmental*, 10, 83-97.
- [16] Farrauto R.J., Voss K.E. (1996). Monolithic diesel oxidation catalysts. *Applied Catalysis B: Environmental*, 10, 29-51.
- [17] Stein H.J. (1996). Diesel oxidation catalysts for commercial vehicle engines: strategies on their application for controlling particulate emissions. *Applied Catalysis B: Environmental*, 10, 69-82.
- [18] Liu S., Obuchi A., Oi-Uchisawa J., Nanba T., Kushiya S. (2001). Synergistic Catalysis of Carbon Black Oxidation by Pt with MoO<sub>3</sub> or V<sub>2</sub>O<sub>5</sub>. *Applied Catalysis B: Environmental*, 30, 259-265.
- [19] Jelles S.J., van Setten B.A.A.L., Makkee M., Moulijn J.A. (1999). Molten Salts as Promising Catalysts for Oxidation of Diesel Soot: Importance of Experimental Conditions in Testing Procedures. *Applied Catalysis B: Environmental*, 21, 35-49.
- [20] Atribak I., Bueno-López A., García-García A., Navarro P., Frías D., Montes M. (2010). Catalytic activity for soot combustion of birnessite and cryptomelane. *Applied Catalysis B: Environmental*, 93, 267-273.
- [21] Aouad S., Saab E., Abi-Aad E., Aboukaïs A. (2007). Study of the Ru/Ce System in the Oxidation of Carbon Black and Volatile Organic Compounds. *Kinetics and Catalysis*, 48, 835-840.
- [22] Aouad S., Saab E., Abi-Aad E., Aboukaïs A. (2007). Reactivity of Ru-based Catalysts in the Oxidation of Propene and Carbon Black. *Catalysis Today*, 119, 273-277.
- [23] Aouad S., Abi-Aad E., Aboukaïs A. (2009). Simultaneous Oxidation of Carbon Black and Volatile Organic Compounds over Ru/CeO<sub>2</sub> Catalysts. *Applied Catalysis B: Environmental*, 88, 249-256.
- [24] Guo M.X., Ouyang F., Pang D.D. and Qiu L. (2013). Highly efficient oxidation of soot over RuOx/SiO<sub>2</sub> in fluidized bed reactor. *Catalysis Communications*, 38, 40-44.
- [25] Rizzi G.A., Magrin A. and Granozzi G. (1999). Substitutional Ti<sub>(1-x)</sub>Ru<sub>x</sub>O<sub>2</sub> Surface Alloys Obtained from the Decomposition of Ru<sub>3</sub>(CO)<sub>12</sub> on TiO<sub>2</sub>(110). *Physical Chemistry Chemical Physics*, 1, 709-711.



- [26] Lanza R., Järås S.G., Canu P. (2007). Partial Oxidation of Methane over Supported Ruthenium Catalysts. *Applied Catalysis A:General*, 325, 57-67.
- [27] Ma L., He D.H. (2010). Influence of Catalyst Pretreatment on Catalytic Properties and Performances of Ru-Re/SiO<sub>2</sub> in Glycerol Hydrogenolysis to Propanediols. *Catalysis Today*, 149, 148-156.
- [28] Ji L., Lin J. and Zeng H.C. (2001). Thermal Processes of Volatile RuO<sub>2</sub> in Nanocrystalline Al<sub>2</sub>O<sub>3</sub> Matrixes Involving  $\gamma \rightarrow \alpha$  Phase Transformation. *Chemistry of Materials*, 13, 2403-2412.
- [29] Zhu R., Guo M., Ci X., Ouyang F. (2008). An exploratory study on simultaneous removal of soot and NO<sub>x</sub> over Ir/ $\gamma$ -Al<sub>2</sub>O<sub>3</sub> catalyst in the presence of O<sub>2</sub>. *Catalysis Communications*, 9, 1184-1188.
- [30] Zhu R., Guo M., Ouyang F. (2008). Simultaneous Removal of Soot and NO<sub>x</sub> over Ir-based Catalysts in the Presence of Oxygen. *Catalysis Today*, 139, 146-151.
- [31] Oi-Uchisawa J., Obuchi A., Enomoto R., Xu J., Nanba T., Liu S., Kushiya S. (2001). Oxidation of Carbon Black over Various Pt/MO<sub>x</sub>/SiC Catalysts. *Applied Catalysis B: Environmental*, 32, 257-268.
- [32] Zhou W., He Y. (2012). Ho/TiO<sub>2</sub> nanowires heterogeneous catalyst with enhanced photocatalytic properties by hydrothermal synthesis method. *Chemical Engineering Journal*, 179, 412-416.
- [33] Tomita K., Petrykin V., Kobayashi M., Shiro M., Yoshimura M., Kakihana M. (2006). A Water-soluble Titanium Complex for the Selective Synthesis of Nanocrystalline Brookite, Rutile, and Anatase by a Hydrothermal Method. *Angewandte Chemie International Edition*, 45, 2378-2381.
- [34] Dong L., Cheng K., Weng W., Song C., Du P., Shen G., Han G. (2011). Hydrothermal Growth of Rutile TiO<sub>2</sub> Nanorod Films on Titanium Substrates. *Thin Solid Films*, 519, 4634-4640.
- [35] Qi B., Wu L., Zhang Y., Zeng Q., Zhi J. (2010). Low-temperature and One-step Synthesis of Rutile TiO<sub>2</sub> Aqueous Sol by Heterogeneous Nucleation Method. *Journal of Colloid and Interface Science*, 345, 181-186.





- [36] Sun J., Gao L. (2002). pH Effect on Titania-phase Transformation of Precipitates from Titanium Tetrachloride Solutions. *Journal of the American Ceramic Society*, 85, 2382-2384.
- [37] Gómez-Cortés A., Díaz G., Zanella R., Ramírez H., Santiago P., Saniger J.M. (2009). Au-Ir/TiO<sub>2</sub> Prepared by Deposition Precipitation with Urea: Improved Activity and Stability in CO Oxidation. *The Journal of Physical Chemistry C*, 113, 9710-9720.
- [38] Tauster S.J., Fung S.C., Garten R.L. (1978). Strong Metal-support Interactions. Group 8 Noble Metals Supported on Titanium Dioxide. *Journal of the American Ceramic Society*, 100, 170-176.
- [39] Haller G.L. and Resasco D.E. (1989), Metal-support Interaction: Group VIII Metals and Reducible Oxides. *Advances in Catalysis*, 36, 173-235.
- [40] Rodríguez-González V., Zanella R., Calzada L.A., Gómez R. (2009). Low-temperature CO Oxidation and Long-term Stability of Au/In<sub>2</sub>O<sub>3</sub>-TiO<sub>2</sub> Catalysts. *The Journal of Physical Chemistry C*, 113, 8911-8917.

#### Graphics captions:

Fig.1 TPR profiles of SiO<sub>2</sub> and Ru/SiO<sub>2</sub> in fluidized bed reactor. Catalyst weight = 0.2 g, soot weight = 0.02 g, feed gas composition= 4.4 vol.% O<sub>2</sub> + Ar, flow rate=150 ml/min

Fig.2 TPR profiles of soot removal over Ru/TiO<sub>2</sub>/SiO<sub>2</sub> calcination at different temperatures in fluidized bed reactor. Catalyst weight = 0.2 g, soot weight = 0.02 g, feed gas composition= 4.4 vol.% O<sub>2</sub> + Ar, flow rate=150 ml/min.

Fig.3 TPR profiles of soot removal over Ru/TiO<sub>2</sub>/SiO<sub>2</sub> for 4TPRs in fluidized bed reactor. Catalyst weight = 0.2 g, soot weight = 0.02 g, feed gas composition= 4.4 vol.% O<sub>2</sub> + Ar, flow rate=150 ml/min.

Fig.4 TPR profiles of Ru/SiO<sub>2</sub> and Pt/SiO<sub>2</sub> in fluidized bed reactor. Catalyst weight = 0.2 g, soot weight = 0.02 g, feed gas composition= 4.4 vol.% O<sub>2</sub> + Ar, flow rate=150 ml/min.

Fig.5 X-ray diffraction patterns of TiO<sub>2</sub>/SiO<sub>2</sub> and Ru/TiO<sub>2</sub>/SiO<sub>2</sub> calcined at different temperatures: (a) TiO<sub>2</sub>/SiO<sub>2</sub> (500 °C), (b) TiO<sub>2</sub>/SiO<sub>2</sub> (600 °C), (c) TiO<sub>2</sub>/SiO<sub>2</sub> (700 °C), (d) Ru/TiO<sub>2</sub>/SiO<sub>2</sub> (500 °C), (e) Ru/TiO<sub>2</sub>/SiO<sub>2</sub> (550 °C), (f) Ru/TiO<sub>2</sub>/SiO<sub>2</sub> (600 °C), (g) Ru/TiO<sub>2</sub>/SiO<sub>2</sub> (650 °C) and (h) Ru/TiO<sub>2</sub>/SiO<sub>2</sub> (700 °C).



Fig.6 H<sub>2</sub>-TPR profiles of (a) SiO<sub>2</sub>, (b) TiO<sub>2</sub>/SiO<sub>2</sub>, (c) Ru/SiO<sub>2</sub> and (d) Ru/TiO<sub>2</sub>/SiO<sub>2</sub>

Fig.7 TEM images of (a) Ru/SiO<sub>2</sub> and (b) Ru/TiO<sub>2</sub>/SiO<sub>2</sub>

Fig.8 TPR profiles of Ru/SiO<sub>2</sub> and Ru/TiO<sub>2</sub>/SiO<sub>2</sub> in fluidized (solid) and fixed bed reactor (open). Catalyst weight = 0.2 g, soot weight = 0.02 g, feed gas composition= 4.4 vol.% O<sub>2</sub> + Ar, flow rate=150 ml/min

**Table captions:**

Table 1. Specific surface areas, pore volume and average pore diameter of samples

Table 2. Catalytic activity of Ru-based catalysts and support oxides for the soot oxidation in fluidized and fixed bed reactors. Catalyst weight = 0.2 g, soot weight = 0.02 g, feed gas composition= 4.4 vol.% O<sub>2</sub> + Ar, flow rate=150 ml/min

**Figures**

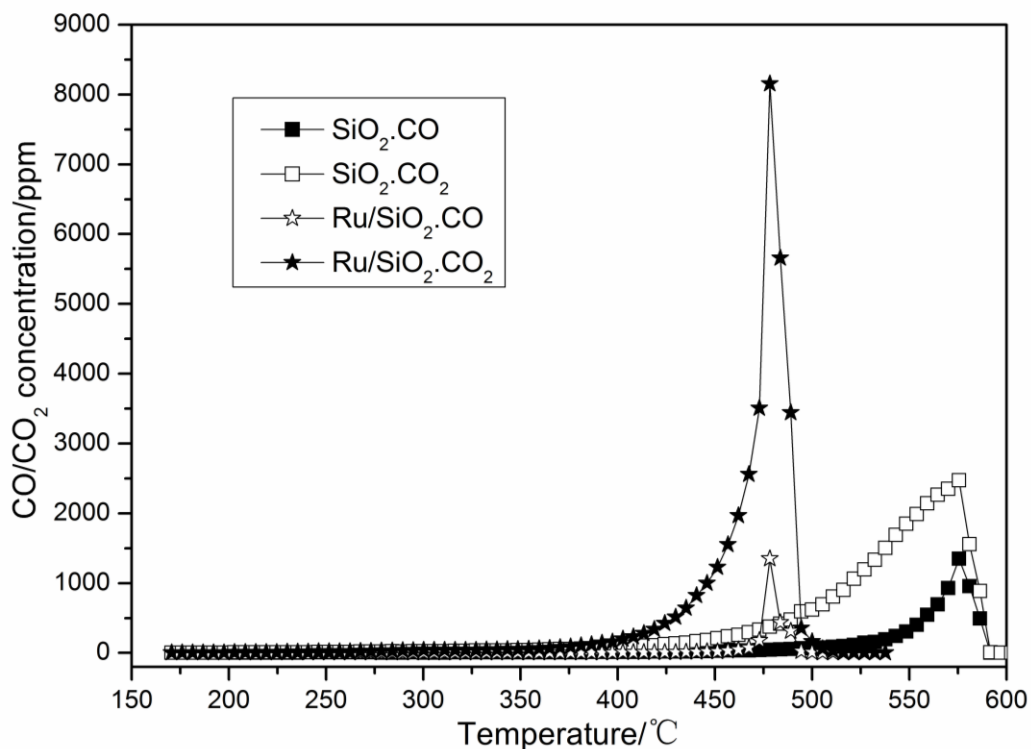


Fig.1 TPR profiles of SiO<sub>2</sub> and Ru/SiO<sub>2</sub> in fluidized bed reactor by Guo *et al.*

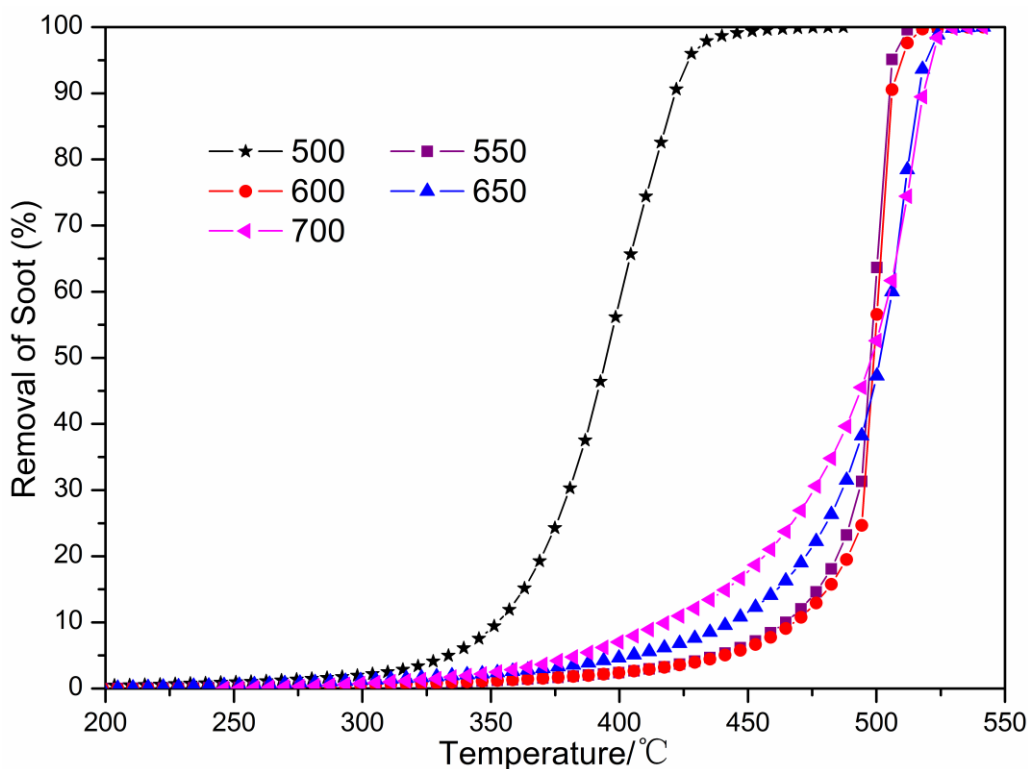


Fig.2 TPR profiles of soot removal over Ru/TiO<sub>2</sub>/SiO<sub>2</sub> calcination at different temperatures in fluidized bed reactor by Guo *et al.*

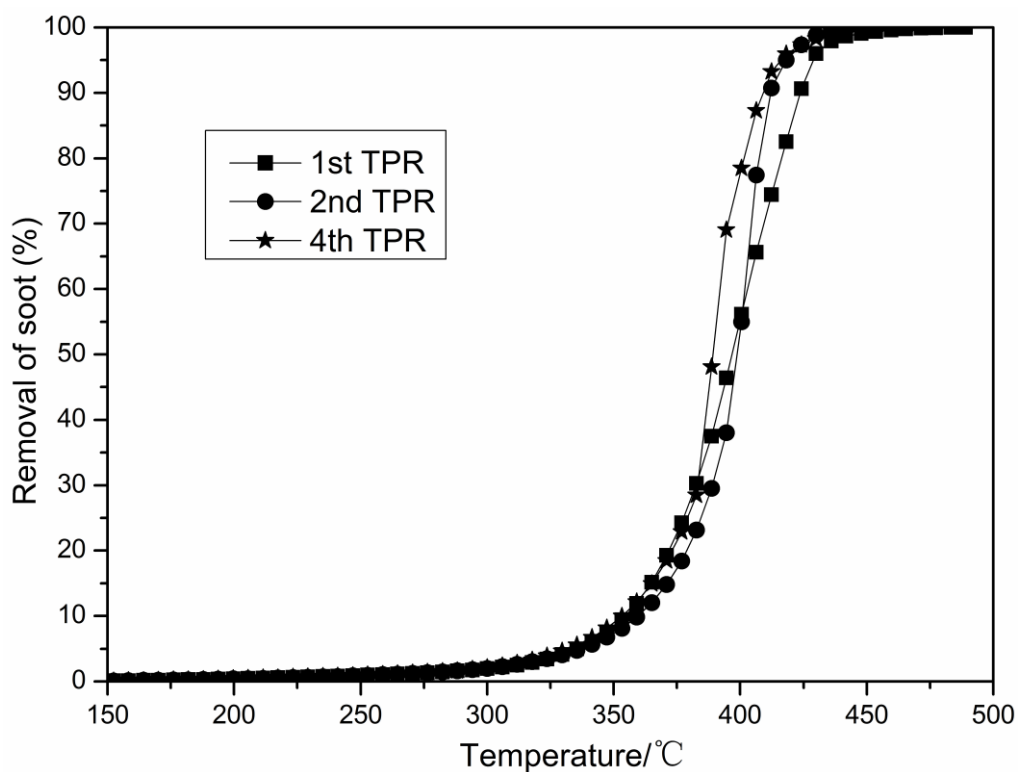


Fig.3 TPR profiles of soot removal over Ru/TiO<sub>2</sub>/SiO<sub>2</sub> for 4 TPRs in fluidized bed reactor by Guo *et al.*

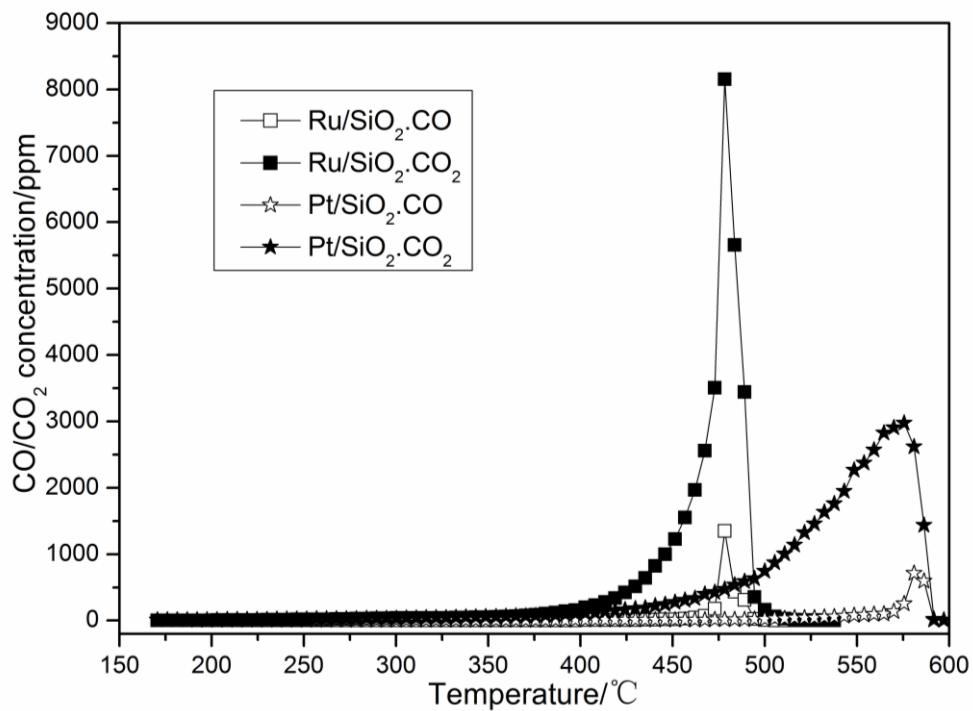


Fig.4 TPR profiles of Ru/SiO<sub>2</sub> and Pt/SiO<sub>2</sub> in fluidized bed reactor by Guo *et al.*

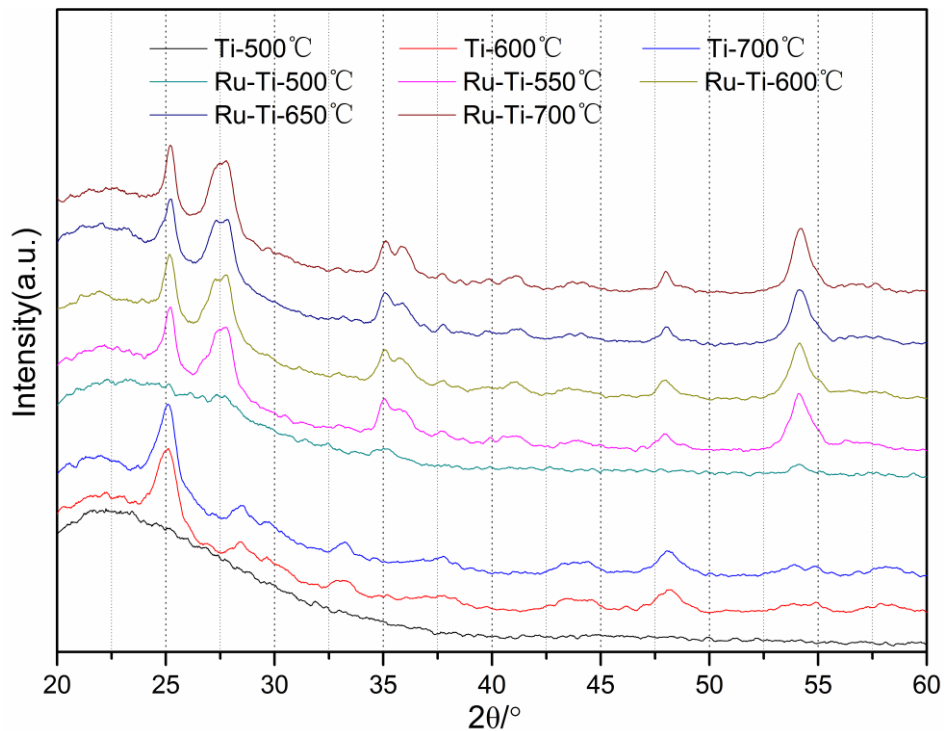


Fig.5 X-ray diffraction patterns of TiO<sub>2</sub>/SiO<sub>2</sub> and Ru/TiO<sub>2</sub>/SiO<sub>2</sub> calcined at different temperatures: (a) TiO<sub>2</sub>/SiO<sub>2</sub> (500 °C), (b) TiO<sub>2</sub>/SiO<sub>2</sub> (600 °C), (c) TiO<sub>2</sub>/SiO<sub>2</sub> (700 °C), (d) Ru/TiO<sub>2</sub>/SiO<sub>2</sub> (500 °C), (e) Ru/TiO<sub>2</sub>/SiO<sub>2</sub> (550 °C), (f) Ru/TiO<sub>2</sub>/SiO<sub>2</sub> (600 °C), (g) Ru/TiO<sub>2</sub>/SiO<sub>2</sub> (650 °C) and (h) Ru/TiO<sub>2</sub>/SiO<sub>2</sub> (700 °C) by Guo *et al.*

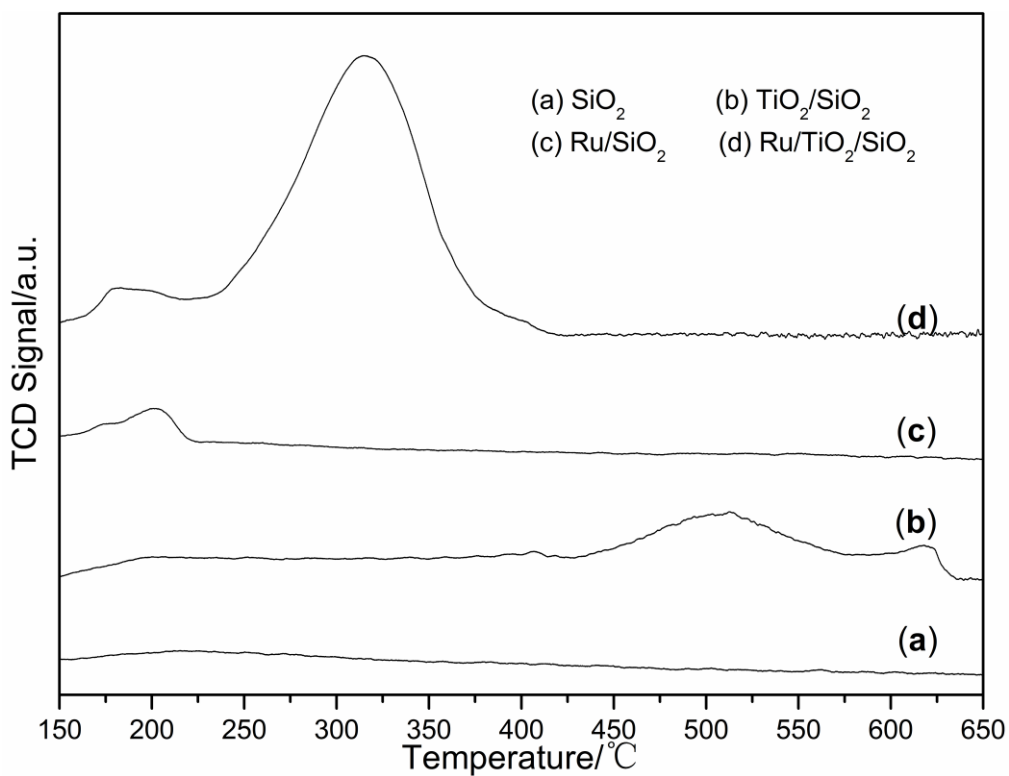


Fig.6  $\text{H}_2$ -TPR profiles of (a)  $\text{SiO}_2$ , (b)  $\text{TiO}_2/\text{SiO}_2$ , (c)  $\text{Ru}/\text{SiO}_2$ , and (d)  $\text{Ru}/\text{TiO}_2/\text{SiO}_2$  by Guo *et al.*

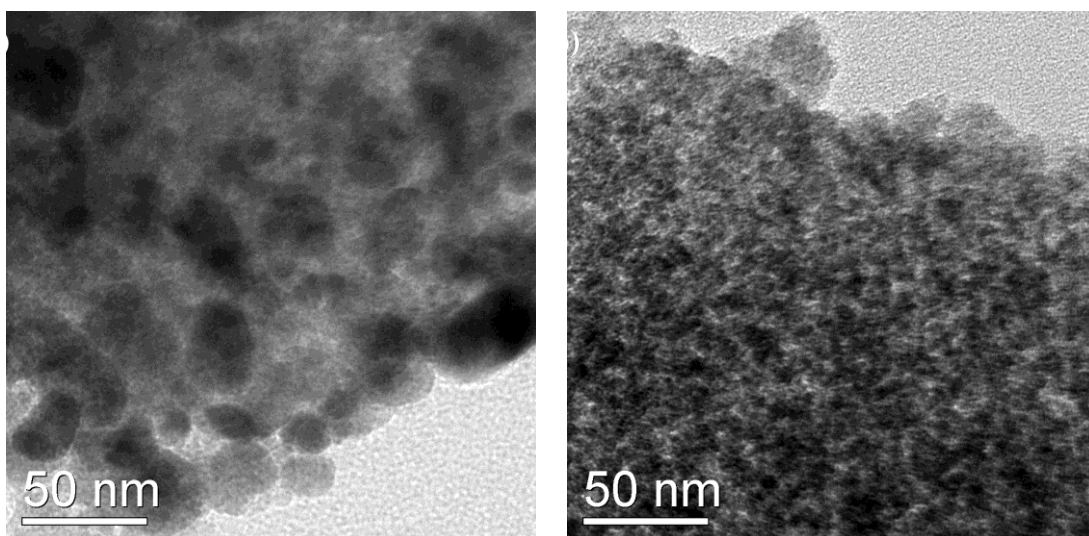


Fig.7 TEM images of (a)  $\text{Ru}/\text{SiO}_2$  and (b)  $\text{Ru}/\text{TiO}_2/\text{SiO}_2$  by Guo *et al.*

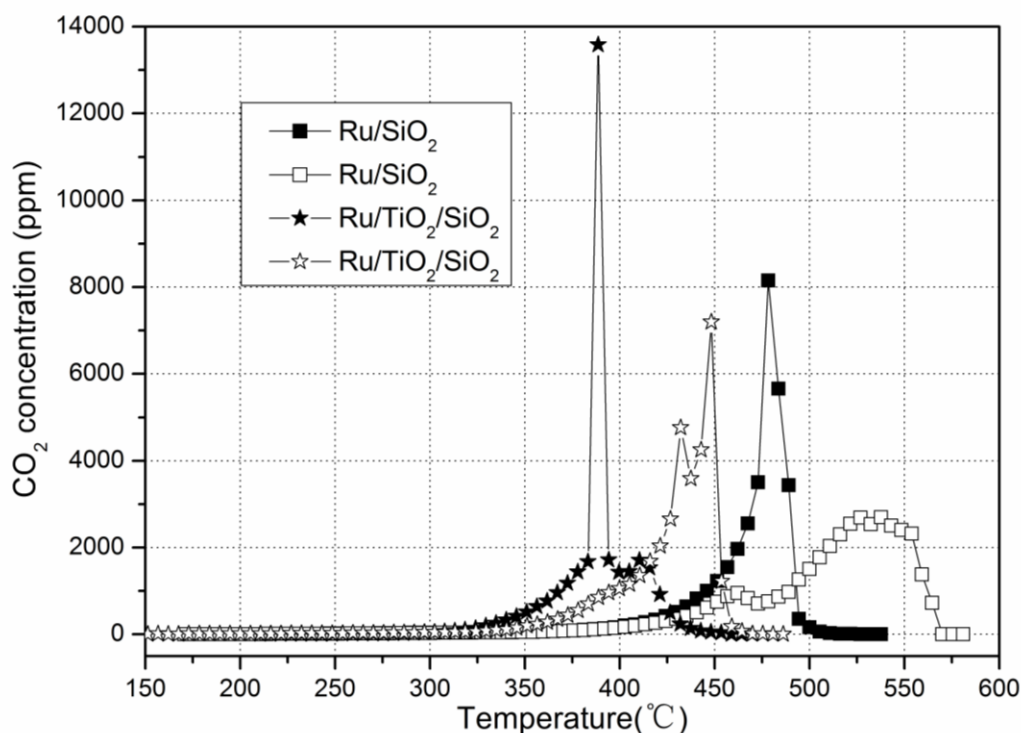


Fig.8 TPR profiles of Ru/SiO<sub>2</sub> and Ru/TiO<sub>2</sub>/SiO<sub>2</sub> in fluidized (solid) and fixed bed reactor (open)

by Guo *et al.*

### Tables

Table 1. Specific surface areas, pore volume and average pore diameter of samples

Catalysts	Specific surface area (m <sup>2</sup> /g)	Total pore volume (cm <sup>3</sup> /g)	Average pore diameter (nm)
SiO <sub>2</sub>	354	1.04	12
Al <sub>2</sub> O <sub>3</sub> /SiO <sub>2</sub>	285	0.71	10
ZrO <sub>2</sub> /SiO <sub>2</sub>	320	0.80	10
TiO <sub>2</sub> /SiO <sub>2</sub>	253	0.62	10
Pt/SiO <sub>2</sub>	353	1.00	11
Ru/SiO <sub>2</sub>	396	1.06	10.8
Ru/Al <sub>2</sub> O <sub>3</sub> /SiO <sub>2</sub>	262	0.67	11
Ru/ZrO <sub>2</sub> /SiO <sub>2</sub>	319	0.85	11
Ru/TiO <sub>2</sub> /SiO <sub>2</sub>	309	0.74	10
TiO <sub>2</sub> /SiO <sub>2</sub> (600 °C)	264	0.76	11
TiO <sub>2</sub> /SiO <sub>2</sub> (700 °C)	244	0.72	12
Ru/TiO <sub>2</sub> /SiO <sub>2</sub> (550 °C)	380	0.88	9
Ru/TiO <sub>2</sub> /SiO <sub>2</sub> (600 °C)	306	0.84	11
Ru/TiO <sub>2</sub> /SiO <sub>2</sub> (650 °C)	305	0.84	11
Ru/TiO <sub>2</sub> /SiO <sub>2</sub> (700 °C)	301	0.86	11



Table 2. Catalytic activity of Ru-based catalysts and support oxides for the soot oxidation in fluidized and fixed bed reactor

Catalysts	Fluidized bed reactor				Fixed bed reactor			
	$T_{10}/^{\circ}\text{C}$	$T_{50}/^{\circ}\text{C}$	$T_{90}/^{\circ}\text{C}$	$S_{\text{co}}/\%$	$T_{10}/^{\circ}\text{C}$	$T_{50}/^{\circ}\text{C}$	$T_{90}/^{\circ}\text{C}$	$S_{\text{co}}/\%$
$\text{SiO}_2$	473	551	579	19.95	476	558	596	32.78
$\text{Al}_2\text{O}_3/\text{SiO}_2$	471	556	591	39.03	492	562	586	24.88
$\text{ZrO}_2/\text{SiO}_2$	492	570	604	46.46	482	559	589	22.98
$\text{TiO}_2/\text{SiO}_2$	491	575	612	53.66	488	566	601	42.67
$\text{Ru}/\text{SiO}_2$	433	475	488	7.24	443	518	552	0.58
$\text{Ru}/\text{Al}_2\text{O}_3/\text{SiO}_2$	421	472	487	5.37	440	505	521	0.89
$\text{Ru}/\text{ZrO}_2/\text{SiO}_2$	437	483	500	3.66	450	509	523	1.1
$\text{Ru}/\text{TiO}_2/\text{SiO}_2$	360	389	414	1.99	382	435	453	2.36